Journal of Photochemistry and Photobiology A: Chemistry 221 (2011) 209–213

Contents lists available at ScienceDirect

Journal of Photochemistry and Photobiology A: Chemistry

journal homepage: www.elsevier.com/locate/jphotochem

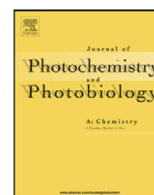

Self-aligned nucleation of gold onto templates with a nano-scale precision fabricated by scanning probe lithography

Hiroyuki Sugimura*, Masao Kanda, Takashi Ichii, Kuniaki Murase

Department of Materials Science and Engineering, Kyoto University, Sakyo, Kyoto 606-8501, Japan

ARTICLE INFO

Article history:
Available online 25 February 2011

Key words:
Self-assembled monolayer
Scanning probe microscopy
Nanolithography
Electroless plating
Gold
Silicon

ABSTRACT

Nanostructures consisting of concentric Au circles with a nm-scale line thickness have been fabricated on silicon (Si) substrates based on electroless plating and by the use of scanning probe microscope as a lithographic tool. First, a micro-template was fabricated on a hexadecyl self-assembled monolayer (HD-SAM) covalently bonded to a Si(1 1 1) substrate by scanning probe anodization lithography in which the HD-SAM was locally degraded and the substrate Si was anodized along a trace of an conductive AFM-tip biased negatively to the grounded Si substrate. Anodic Si oxide formed by this local anodization process was then etched with HF in order to expose the Si surface under the anodic oxide layer. Consequently, a Si nanopattern surrounded with the HD-SAM identical to the anodic oxide pattern was formed. This Si nanopattern served as a template for fabricating a Au nanostructure by means of electroless plating. Due to the galvanic displacement of surface Si atoms with Au complex ions in a plating bath, Au started to nucleate on the exposed Si surface, while no nuclei was formed on the surrounding HD-SAM. Consequently, a Au nanostructure was formed through further Au deposition on the Au nuclei. The fabricated Au nanostructures are promising for applications emerging plasmonic functions.

© 2011 Elsevier B.V. All rights reserved.

1. Introduction

Nanostructures consisting of metals are expected to emerge a variety of functions adaptable in, for example, electronic, photonic, magnetic, chemical and biological applications [1,2]. Among various metals, gold (Au) are of primary importance due to its photonic applications based on plasmonic activities of Au. Furthermore, Au is advantageous, since its surface can be readily modified with an organic monolayer having a particular function through chemical affinities of Au toward some types of chemical functional groups. Furthermore, two-dimensional Au nanopatterns are of particular interest owing to their unique photonic functions [3].

Scanning probe lithography in which scanning probe microscopy is employed as a lithographic tool, has been recognized as convenient for creating nanopatterns on a solid substrate [4–7]. Indeed, the method has been successfully applied to fabricated metallic nanostructures. For example, onto nano-scale templates prepared scanning probe lithography, pre-synthesized metal nanoparticles have been area-selectively arranged resulting in the formation of two-dimensional nanoparticle arrays [8–12]. Moreover, electroless plating has been employed as a pattern transfer process in order to fabricate metal nanostructures, e.g., Ni, Cu, Au and so forth, from two-dimensional patterns drawn by scanning probe lithography [13–15]. In this case, metal nanostructures with a more sophisticated design can be fabricated.

In this paper, we report on the fabrication of Au nanostructures on silicone (Si) by means of electroless plating with the spatial control of nucleation site. A two-dimensional pattern has been first drawn on a Si substrate covered with an alkyl self-assembled monolayer (SAM) by the use of atomic force microscope (AFM). Then, the sample surface is prepared by chemical etching in order to define the nucleation site. Finally, the sample is treated in a Au plating bath. Consequently, Au deposit selectively on the area where has been scanned by the AFM-tip.

There are two particular aims in this research. The first aim of this research is to elucidate the pattern transfer process through electroless plating. Since electroless nucleation of Au on Si has been found to initiate at certain nucleation sites, mainly at step edges, consequently, at the beginning of plating, deposited Au does not form a continuous film but form an ensemble of nanoparticles [20]. Thus, plating conditions are needed to be optimized in order to fabricate continuous Au nanolines as well as to confirm how accurately can we transfer anodic oxide patterns to Au patterns. The second aim is to confirm the accuracy of patterning and plating. Although there are some advantages and disadvantages in scanning probe lithography, the most essential advantage of scanning probe lithography is its potential on high pattern alignment accuracy. Since a sample surface can be imaged without modifying its

* Corresponding author. Tel.: +81 75 753 9131, fax: +81 75 753 4861.
E-mail address: hiroyuki-sugimura@mtl.kyoto-u.ac.jp (H. Sugimura).

1010-6030/$ – see front matter © 2011 Elsevier B.V. All rights reserved.
doi:10.1016/j.jphotochem.2011.02.018

surface based on scanning probe microscopy, additional patterns can be drawn on the sample surface using the pre-obtained sample image as a map [16]. This advantage of scanning probe lithography cannot be available in other lithographies including electron beam lithography in which a sample surface cannot be imaged without exposing a resist film covering the sample surface. However, due to nonlinearities of a PZT scanner, patterns drawn by scanning probe lithography frequently distorted. In this case, the advantage of scanning probe lithography cannot be brought into full scope, so that we have employed a closed loop scanner in order to reduce distortions. We have constructed circular grating structures, since such structures are favorable for the demonstration of patterning accuracy and, besides unique functions due to the coupling of optical diffraction and surface plasmon [17–20].

2. Sample preparation – Si covered with an alkyl monolayer

Substrates cut from a phosphorus-doped n-type Si(1 1 1) wafer [resistivity; 1–10 Ωcm, thickness; ca. 500 μm, offangle; <0.5°] were first sonicated in ethanol and in pure water in that order for 20 min each. These washed substrates were further treated by an optical cleaning method using vacuum ultra-violet light at 172 nm in wavelength in order to remove residual organic contamination and to complete covering the Si substrates with a thin and clean surface oxide layer [21]. Next, the surface oxide layer on the substrates was removed and their surfaces were terminated with hydrogen with the procedure as described below. The oxide-covered Si substrates were etched in 5% HF for 5 min at room temperature. Then, the substrates placed in dark were immersed in 40% NH_4F for 30 s at a temperature of 80 °C.

An alkyl SAM of the hexadecyl form ($Si\text{-}C_{16}H_{33}$) was covalently fixed on the hydrogen-terminated Si (Si(1 1 1)-H) substrates through a photo activation process [22]. Each Si(1 1 1)-H sample was placed in a reaction cell made of quartz filled with neat 1-hexadecene ($H_2C{=}CH(CH_2)_{13}CH_3$, Tokyo Kasei Co. Ltd.). The 1-hexadecene liquid was deairated with bubbling of a continuous flow of nitrogen for 30 min. Then, with continuing nitrogen bunling, the Si(1 1 1)-H substrate was illluminated for 1 h with 250 W super high pressure murcury lamp (Asahi Spectra Co. Ltd., REX-250) with a prower density of 100 mW cm^{-2} regulated using a ND filter system equiped in the lamp house. After this photo irradiation, the sample was taken out from the quartz cell and, then, was rinsed thoroughly using hexane, ethanol, and ultra pure water in that order each for 10 min. It was confirmed by ellipsometry (Otsuka Electronics Co. Ltd., FE-5000) that a film of 2.3 nm in thickness, which corresponds to the thickness of the hexadecyl monolayer on Si [22], was formed on the substrate. The water contact angle of the monolayer-formed Si sample was found to be 107°. Fig. 1 shows

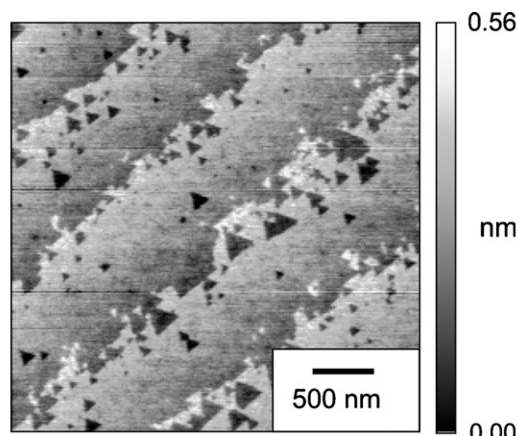

Fig. 1. AFM image of a Si(1 1 1) surface covered with a HD-SAM.

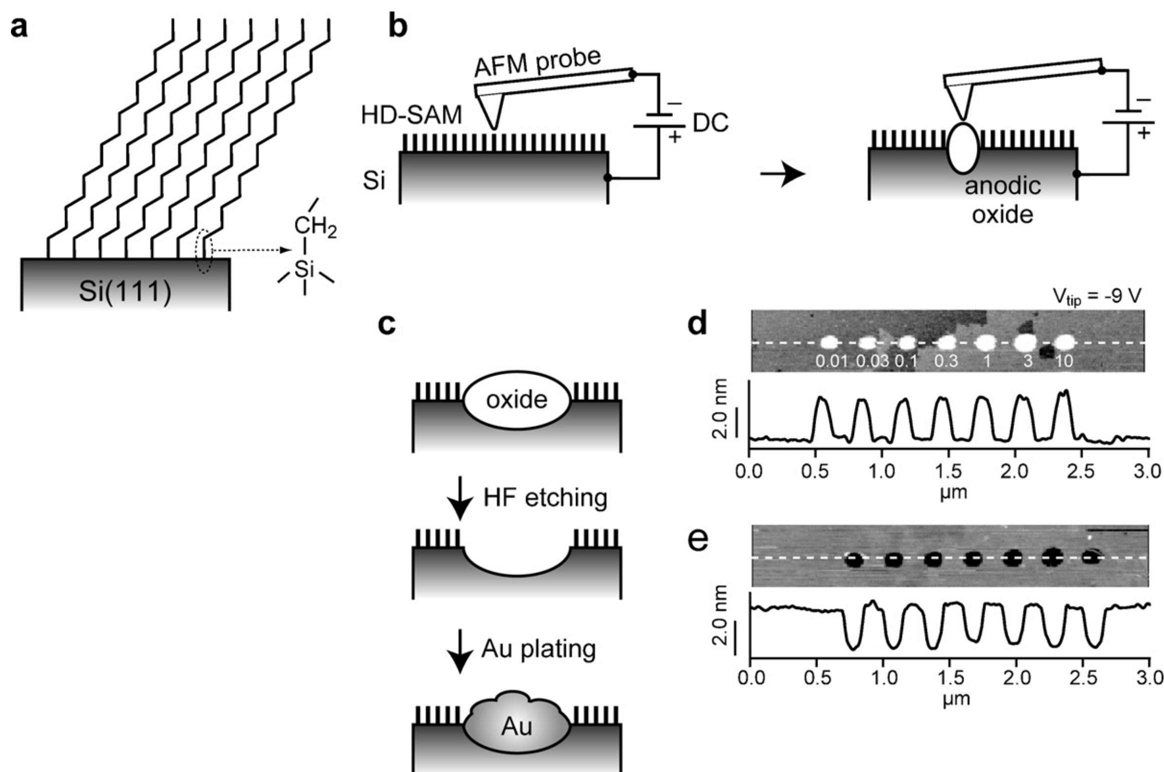

Fig. 2. Fabrication process for Au nanostrucures. (a) HD-SAM/Si sample, (b) scanning probe anodization lithography, (c) chemical process for attaining area-selective Au deposition, (d) AFM image and its cross section of anodized dots and (e) AFM image and its cross section of etched holes.

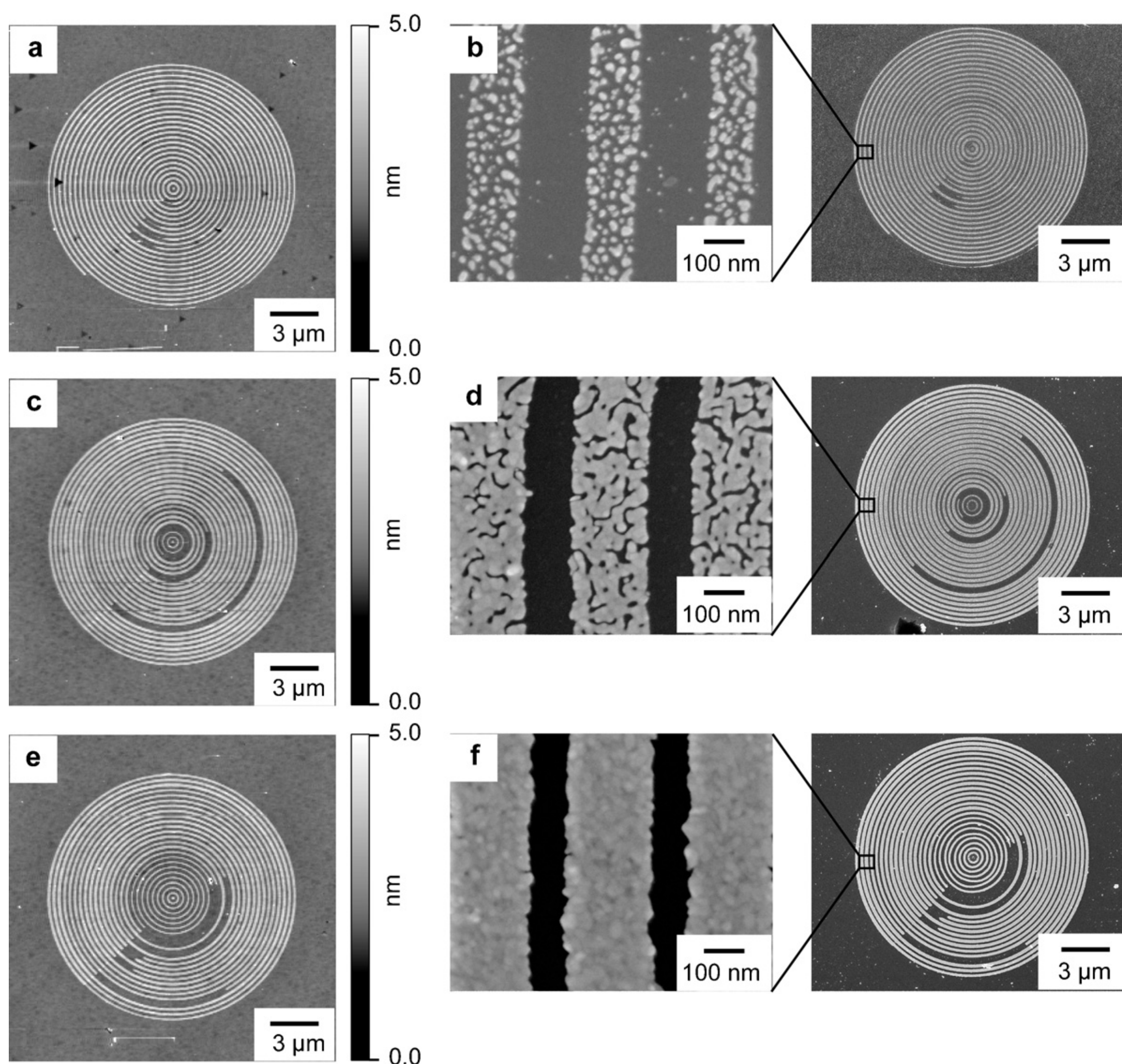

Fig. 3. Au circles fabricated with varied plating times. (a) AFM image of anodized circles served for 1-min plating. (b) FE-SEM images of Au circles plated for 1 min on the template fabricated from the sample (a). (c) AFM image of anodized circles served for 5-min plating. (d) FE-SEM images of Au circles plated for 5 min on the template fabricated from the sample (c). (e) AFM image of anodized circles served for 10-min plating. (f) FE-SEM images of Au circles plated for 1 min on the template fabricated from the sample (e).

a typical morphology of the sample surface. There are monoatomic steps of 0.3 nm high separating flat terraces and triangular etch pits of 0.3 nm in depth. These sub-nm high features are peculiar to the Si(1 1 1)-H substrate surface before depositing the monolayer. Namely, the features are preserved on the monolayer surface, even though its thickness is nearly 10 times of the heights of the features. These results suggest that the monolayer has been conformally formed on the Si substrate.

3. Patterning – template preparation for Au plating

Patterns were drawn on a Si substrate covered with a hexadecyl SAM (HD-SAM) (Fig. 2a) by scanning probe anodization lithography [23,24]. As schematically illustrated in Fig. 2b, a negative bias was applied to an electrically conductive tip of atomic force microscope (AFM), while the Si substrate served as a counter electrode connected to ground. In this study, we used an AFM equipped with a closed loop horizontal scanner (Asylum Research, MPF-3D) was used in order to attain pattern drawing without distortions due to nonlinearities of a PZT scanner. An AFM probe made of Si coated with Rh (SII NanoTechnology, Inc., SI-DF3-R) was used. During patterning, the AFM was operated in the contact mode. As schematically illustrated in Fig. 2c, anodic oxidation with adsorbed water is promoted at the AFM-tip junction so that, around the junction, the organic monolayer is degraded and the substrate Si is anodized to Si oxide. Accordingly, the area where current has been injected from the AFM tip protrudes. Fig. 2d shows an AFM image and its cross section of an example for this nanofabrication process. There are 7 dots protruded nearly 2 nm from the surrounding area. These dot features were fabricated at an AFM tip bias of −9 V. A bias duration time was varied from 0.01 to 10 s as indicated in Fig. 2d. Since the anodic reactions at the AFM-tip/sample junction are promoted with adsorbed water, the control of relative humidity is crucial to attain reproducible patterning. For example, line width becomes thicker with an increase in humidity. A slower probe scan rate is required in order to complete anodization when a humidity is too low. In this research, a relative humidity for scanning probe anodization was regulated to be more than 60%.

The locally anodized sample is then etched with 0.5% HF for 5 min at room temperature in dark. Since the HD-SAM bonded to Si is not etched due to the chemical durability of Si–C bond to HF [25], only anodic oxide is etched. The anodic oxide dots shown in Fig. 2d became holes about 2 nm in depth as shown in Fig. 2e.

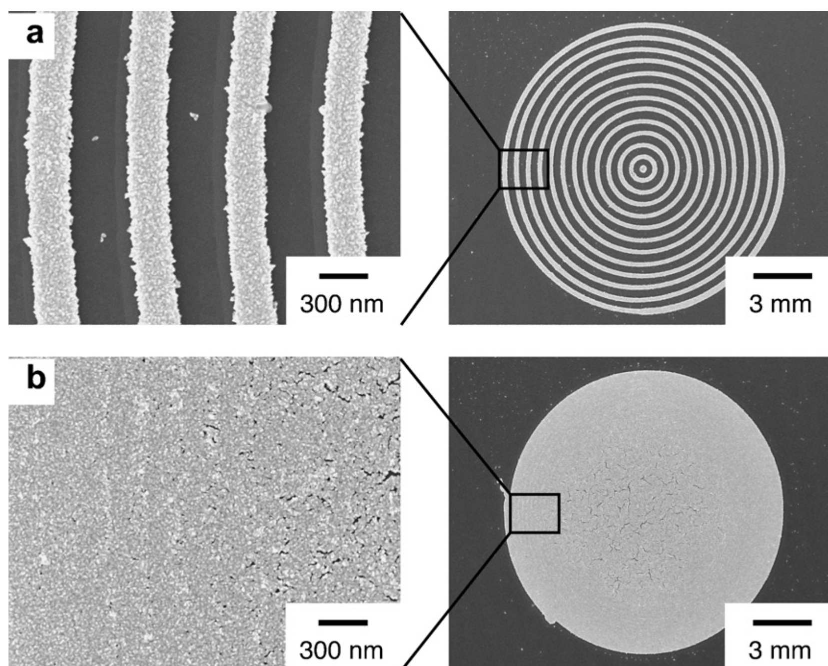

Fig. 4. FE-SEM images of (a) Au mult-ring and (b) Au disk samples.

4. Au nanostructures fabricated on the templates

The template prepared by scanning probe anodization and HF etching was immersed in an electroless Au plating bath (Kojundo Chemical Laboratory Co., K-24S) for an appropriate time. The sample was then rinsed with pure water and then blown dry. Since in this plating bath, Au nucleates on Si due to the galvanic displacement of surface Si atoms with Au complex ions in solution, while such a reaction does not proceed on the region covered with the HD-SAM, Au deposits only in the region where oxide had been etched away as illustrated in Fig. 2c. Consequently, a pattern drawn by AFM is transferred to a structure consisting of Au.

The Au-plated samples were characterized by the same AFM used for patterning and a field-emission scanning electron microscope (FE-SEM, JEOL Ltd., JSM-6500F). In addition, optical reflectance spectra of Au nanostructures formed on the samples were aquired by a micro spectroscopy measurement system constructed from an optical microscope (Nikon Co., Eclipse MCPD-7700) and a multi channel photo detector system (Otsuka Electronics Co., MPD-7700). Using a 20× objective lense, reflected light form a micro spot of 10 μm in diamer on a sample surface was measured. The sample surface was illuminated with a halogen lamp of the microscope. Measurements were conducted in the wavelength range of 450–900 nm with an exposure time of 100 ms and an accumulation number of 100.

First, we have optimized the plating period. As shown in Fig. 3a, c and e, a pattern consisting of 24 concentric circles with a maximum diameter of 15 μm on each of HD-SAM/Si (Si-HD) samples was drawn using a Rh-coated AFM tip at a bias of −8 V with a tip-scan rate of 500 nm/s. Environmental temperature and relative humidity were room temperature and 60%, respectively. Although there are some defects, all the circles are accurately aligned concentrically at a same interval in each of the patterns. Each circle has started to be drawn form its top. Thus, it can be confirmed from the AFM images that the starting and ending points for circle drawing are coincident. Patterning has been sufficiently accurate and precise to create nanostructures.

These three patterned samples were treated through the surface modification procedure, that is, HF etching and Au electroless plating, as illustrated in Fig. 2c. The resulted samples with a plating time at 1, 5 and 10 min were observed by FE-SEM. Results are shown in Fig. 3b, d and f, respectively. The bright regions in these images correspond to the region where Au had been deposited. The anodic oxide patterns including the defects are transferred to the concentric-circle patterns of Au.

We have reported previously that, in electroless plating of Au on Si, nucleation did not proceed uniformly on Si(1 1 1) surface but started at particular sites, e.g., step edges and etch pits [24,26]. When plating was prolonged, the Au nuclei continued to glow through a catalytic process and finally connected each other to form a continuous Au film. Identical to this conclusion, at a plating time of 1 min, the deposited Au does not form continuous films as can be seen in a magnified FE-SEM image shown in Fig. 3a. The Au nucleation on the Si surface exposed by HF etching seems to be initiated at certain sites. At this plating time, the nucleation area is identical to the area where anodized by AFM, that is, lines of 120 nm wide. The height of the Au deposits is about 12 nm as confirmed by AFM. At a plating time of 5 min, Au nuclei have further grown so as to merge each other although there remains gaps between the merged Au islands, as shown in a magnified FE-SEM image of Fig. 3d. The deposit height increased up to about 16 nm. In contrast to this slight growth of the Au deposits to the vertical direction, the Au islands have more markedly grown horizontally. The width of the Au deposition lines becomes to be 190 nm. The width of the original anodized lines as shown in Fig. 3c are nearly same with that of the anodized lines as shown in Fig. 3a, i.e., 120 nm. This result indicates that Au deposition was expanded from the anodized area to its outside. This is most likely because plating proceeds isotropically. As demonstrated in Fig. 1e, the depth etched with HF is only a few nm so that Au starts to grow horizontally when the deposition thickness is exceeded this etched depth. At a plating time of 10 min, we could fabricate continuous Au lines as demonstrated in Fig. 3f. Their height and width are 25 and 220 nm, respectively.

We have successfully fabricated a multi-microring sample consisting of continuous lines without defects as shown in Fig. 4a under optimized fabrication parameters. This 12-ring pattern with a maximum diameter of 15 μm was drawn at AFM-tip bias and scan rate of −9 V and 300 nm/s, respectively. A relative humidity of environ-

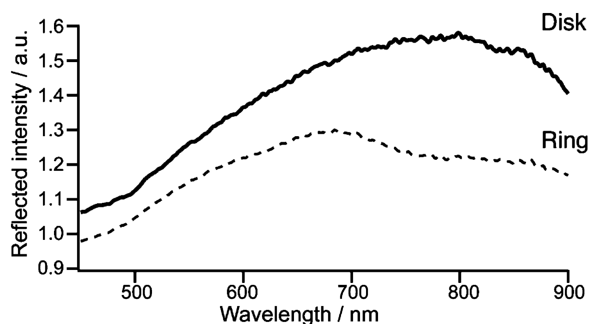

Fig. 5. Reflectance spectra of the Au mult-ring and disk samples.

ment was about 70%. Etching was conducted for 5 min with 0.5% HF in dark and Au plating was done for 10 min at a bath temperature of 30 °C. Widths of the Au lines are estimated to be about 210 nm from the FE-SEM image. As a control sample, we also fabricated an Au disk of 15 μm in diameter by densely scanned with the biased AFM-tip as shown in Fig. 4b. Optical reflectance spectra of these two Au microstructures are shown in Fig. 5. Each spectrum was measured at the center part of 10 μm in diameter and normalized by a reflectance spectrum of Si-HD surface without Au deposits. A maximum of the relative reflectance ($R_{Au}/R_{Si\text{-}HD}$) of the Au disk is about 1.6, which is larger than that of the Au multi-ring, that is, 1.3. This difference corresponds to the difference in area coated with Au on the both sample surfaces. Besides the maximum value, there are distinct difference in peak wavelengths between the spectra. The reflectance is peaked at around 800 nm in wavelength for the Au disk, while that of the Au multi-ring shows its peak at 680 nm in wavelength. This peak wavelength difference might be caused by plasmonic effects. Since, in the Au multi-ring, Au is structured into nanolines, its reflectance peak is positioned at the shorter wavelength, as similarly to the blue shift of plasmonic peak wavelength appeared when Au nanoparticles become smaller.

5. Conclusion

Micro-ring structures consisting of concentric circles with a nm-scale wide line made of Au have been fabricated on Si substrates. A templates was first fabricated on a Si-HD substrate by scanning probe anodization lithography. This anodized pattern was transferred to a Au pattern by HF etching followed by Au electroless plating. The fabricated Au micro-rings consisting of nano-scale wide lines are expected to be applied as elements for coupling optical diffraction and plasmonic functions and by JOINT TAIWANESE -JAPANESE RESEARCH GRANT from Japan Science and Technology Agency.

Acknowledgements

This work was supported by KAKENHI (Grant-in-Aid for Scientific Research) No. 19049010 on Priority Area “Strong Photons-Molecules Coupling Fields (470)” from the Ministry of Education, Culture, Sports, Science and Technology of Japan.

References

[1] A.N. Shipway, E. Katz, I. Willner, ChemPhysChem 1 (2000) 18.
[2] K. Kneipp, H. Kneipp, J. Kneipp, Acc. Chem. Res. 39 (2006) 443.
[3] K. Ueno, S. Juodkazis, T. Shibuya, Y. Yokota, V. Mizeikis, K. Sasaki, H. Misawa, J. Am. Chem. Soc. 130 (2008) 6928.
[4] H. Sugimura, N. Nakagiri, Jpn. J. Appl. Phys. 34 (1995) 3406.
[5] C.F. Quate, Surf. Sci. 386 (1997) 259.
[6] D. Wouters, U.S. Schubert, Angew. Chem. Int. Ed. 43 (2004) 2480.
[7] R. Garcia, R.V. Martinez, J. Martinez, J. Chem. Soc. Rev. 35 (2006) 29.
[8] J. Zheng, Z. Zhu, H. Chen, Z. Liu, Langmuir 16 (2000) 4409.
[9] S. Liu, R. Maoz, J. Sagiv, Nano Lett. 4 (2004) 845.
[10] Z.M. Fresco, J.M.J. Fréchet, J. Am. Chem. Soc. 127 (2005) 8302.
[11] S.-D. Tzeng, K.-J. Lin, J.-C. Hu, L.-J. Chen, S. Gwo, Adv. Mater. 18 (2006) 1147.
[12] O.M. Khatri, J. Han, T. Ichii, K. Murase, H. Sugimura, J. Phys. Chem. C 112 (2008) 16182.
[13] H. Sugimura, N. Nakagiri, Appl. Phys. Lett. 66 (1995) 1430.
[14] S.L. Brandow, J.M. Calvert, E.S. Snowand, P.M. Campbell, J. Vac. Sci. Technol. A 15 (1997) 1455.
[15] H. Sugimura, O. Takai, N. Nakagiri, J. Electroanal. Chem. 473 (1999) 230.
[16] H. Sugimura, N. Nakagiri, Appl. Phys. A 66 (1998) S427.
[17] H.J. Lezec, A. Degiron, E. Devaux, R.A. Linke, L. Martin-Moreno, F.J. Garcia-Vidal, T.W. Ebbesen, Science 297 (2002) 820.
[18] T. Ishi, J. Fujikata, K. Makita, T. Baba, K. Ohashi, Jpn. J. App. Phys. 44 (2005) L364.
[19] A. Kubo, Y.S. Jung, H.K. Kim, H. Petek, J. Phys. B: At. Mol. Opt. Phys. 40 (2007) S259.
[20] X. Cui, K. Tawa, K. Kintaka, J. Nishii, Adv. Func. Mater. 20 (2010) 945.
[21] H. Sugimura, A. Hozumi, T. Kameyama, O. Takai, Surf. Interface Anal. 34 (2002) 550.
[22] H. Sano, H. Maeda, S. Matsuoka, K.-H. Lee, K. Murase, H. Sugimura, Jpn. J. Appl. Phys. 47 (2008) 5659.
[23] H. Sugimura, N. Nakagiri, Langmuir 11 (1995) 3623.
[24] H. Sugimura, S. Nanjo, H. Sano, K. Murase, J. Phys. Chem. C 113 (2009) 11643.
[25] H. Sano, H. Maeda, T. Ichii, K. Murase, K. Noda, K. Matsushige, H. Sugimura, Langumuir 25 (2009) 5516.
[26] S. Yae, N. Nasu, K. Matsumoto, T. Hagihara, N. Fukumuro, H. Matsuda, Electrochim. Acta 53 (2007) 35.